EPJ manuscript No.
(will be inserted by the editor)

Prospects of Open Charm Production at GSI-FAIR and J-PARC

J. Riedl[1], A. Schäfer[1] and M. Stratmann[2]
[1] Institut für Theoretische Physik, Universität Regensburg, D-93040 Regensburg, Germany
[2] Radiation Laboratory, RIKEN, 2-1 Hirosawa, Wako, Saitama 351-0198, Japan

Abstract. We present a detailed phenomenological study of the prospects of open charm physics at the future $\bar{p}p$ and pp facilities GSI-FAIR and J-PARC, respectively. In particular, we concentrate on differential cross sections and the charge and longitudinal double-spin asymmetries at next-to-leading order accuracy. Theoretical uncertainties for the proposed observables are estimated by varying the charm quark mass and the renormalization and factorization scales.

PACS. 12.38.Bx – 13.88.+e

1 Motivation and Introduction

In recent years, the study of heavy flavors at colliders has become a versatile tool to probe different aspects of Quantum Chromodynamics (QCD), ranging from heavy flavor parton densities and the hadronization of heavy quarks into heavy mesons or baryons to the dynamics of QCD hard-scattering [1]. Technological advances, like the introduction of micro-vertex detectors, allow for much better tagging of the produced heavy quarks and hence more precise measurements. An equally significant improvement of the theoretical foundations for heavy flavor production has been achieved, in particular, novel proposals to overcome limitations of fixed-order calculations and to model the hadronization of heavy quarks more reliably [1]. As a consequence, a discrepancy between data and theory for bottom production, suggested by various experiments, has been reduced to the point that it no longer appears significant [2].

A solid understanding of the theoretical framework for heavy quark production and its phenomenological inputs is of utmost importance for several key measurements both ongoing or taking place in the very near future [1]. At the LHC, heavy flavor production by genuine QCD processes is an important background to searches for Higgs bosons within the Standard Model and beyond, e.g., to the decay $H \to b\bar{b}$, as well as for new physics. At the Relativistic Heavy Ion Collider (RHIC) one wants to establish the existence and to investigate the properties of a new state of matter, the quark-gluon plasma (QGP). Several signatures related to heavy flavors have been proposed, in particular, how their production and decays are modified by the presence of a QGP [3]. Here, heavy flavor production in proton-proton collisions will act as a benchmark for possible modification in nucleus-nucleus collisions at the same energy [3,4]. In addition, RHIC is also capable to collide longitudinally polarized protons at center-of-mass system (c.m.s.) energies of up to $\sqrt{S} = 500\,\mathrm{GeV}$. Besides its intrinsic interest as an important test of the dynamics of spin-dependent hard-scattering in QCD, these measurements are likely to further our understanding of how gluons contribute to the proton spin, a major goal of hadron physics [5].

In terms of perturbative QCD (pQCD), relevant fixed-order calculations have been in place for quite some time now, and next-to-leading order (NLO) accuracy is the state-of-the-art throughout. NLO results, which keep the full dependence on the heavy quark mass m_Q, for unpolarized hadron-hadron ("hadroproduction"), photon-hadron ("photoproduction"), and electron-hadron ("electroproduction") collisions can be found in [6], [7], and [8], respectively. Calculations for longitudinally polarized hadro- [9] and photoproduction [10] are more recent achievements. In each case one exploits the fact that m_Q acts as an effective infrared cut-off for collinear singularities, which allows to compute total heavy quark yields as a perturbative series in the strong coupling α_s evaluated at a hard scale of $\mathcal{O}(m_Q)$. For inclusive transverse-momentum p_T distributions, complications arise once $p_T/m_Q \gg 1$, and large logarithms in this ratio have to be resummed to all orders in α_s to improve the convergence of the perturbative series [11].

In this paper, we will focus on a detailed phenomenological study of the prospects of open charm production in $\bar{p}p$ and pp collisions at the future GSI-FAIR [12] and J-PARC [13] facilities, respectively. For GSI-FAIR we consider the so-called "collider option" as proposed by the PAX collaboration [14], using a 15 GeV anti-proton and a 3.5 GeV proton beam, with the plan of having both beams also longitudinally or transversely polarized. The main goal of the PAX experiment would be a determination of the so far unknown "transversity" parton densities through the transversely polarized Drell-Yan process.

This measurement would gain substantially from a polarized anti-proton beam due to the dominance of the lowest order (LO) quark-antiquark annihilation channel. The J-PARC facility in Japan is currently being completed. Here we consider the collision of a 50 GeV proton beam with a fixed, solid-state target. The possibility of having both beam and target polarized is a conceivable option for future upgrades currently being scrutinized. At GSI-FAIR (J-PARC) the available $\bar{p}p$ (pp) c.m.s. energy will be $\sqrt{S} \simeq 14.5\,(10)\,\mathrm{GeV}$. For both experiments the details of the detector and the acceptance are not yet finalized. We will make some reasonable assumptions as stated below in Sec. 3.1. We will demonstrate that measurements of open charm at these facilities have the potential to further our understanding of the underlying QCD dynamics at moderate c.m.s. energies so far little explored.

First, one has to determine, of course, to what extent perturbative QCD is applicable at c.m.s. energies of about 10 to 15 GeV. NLO calculations for single-inclusive p_T-spectra of pions or photons are known to seriously undershoot data even at somewhat higher c.m.s. energies [15]. The mass of the charm quark already sets a hard scale of $\mathcal{O}(1\,\mathrm{GeV})$, which may facilitate the use of perturbative QCD even for small or vanishing transverse momenta p_T of the observed charm quark. Also, since $p_T \approx \mathcal{O}(m_Q)$, we do not have to worry about potentially large logarithms $\ln p_T/m_Q$ present at large c.m.s. energies [11], however, partonic threshold effects may become important and perhaps need to be resummed to all orders. In case of p_T-differential pion spectra, it was shown that threshold resummations can lead to a much improved agreement between theory and experiment at low c.m.s. energies [15]. To study the possible relevance of resummations at GSI-FAIR and J-PARC, we provide total and differential charm yields for both $\bar{p}p$ and pp collisions at NLO accuracy of QCD, including detailed discussions of theoretical uncertainties due to variations of the charm quark mass or the renormalization and factorization scales. We note that the computation of threshold resummations for charm production at GSI-FAIR and J-PARC is far beyond the scope of this paper, which aims at a first exploratory study of charm physics at comparatively low c.m.s. energies.

Other interesting, though experimentally more challenging observables related to open charm production can be considered at GSI-FAIR and J-PARC. One is the so called "charge asymmetry" which describes the difference of cross sections for producing a heavy quark Q or a heavy anti-quark $\bar{Q}$ at a certain point in phase-space:

$$A_C \equiv \frac{d\sigma^Q - d\sigma^{\bar{Q}}}{d\sigma^Q + d\sigma^{\bar{Q}}} \quad . \tag{1}$$

This asymmetry probes a subset of NLO radiative corrections and vanishes at the LO approximation. This feature makes it an important test of QCD hard scattering dynamics. The Abelian (QED) part of A_C is also known as forward-backward asymmetry [16] and is caused by the interference of states with different C-parity. It should be mentioned that routinely used event generators based on LO matrix elements cannot predict this interesting effect. In the unpolarized case the charge asymmetry was first mentioned in [17,6] and later studied qualitatively in [18, 19], mainly for top production at the TeVatron and the LHC. A first measurement of A_C for top production has been recently reported by the CDF collaboration [20]. We estimate the size of this effect for GSI-FAIR and J-PARC and, for the first time, compute the corresponding charge asymmetry also for polarized hadroproduction. We will give more details in Sec. 2.2.

Provided that longitudinally polarized beams and targets will be available at GSI-FAIR and/or J-PARC, studies of the double-spin asymmetry

$$A_{LL} \equiv \frac{d\Delta\sigma}{d\sigma}. \tag{2}$$

could provide unique insight in the distributions describing the polarization of quarks and gluons in the nucleon at medium-to-large momentum fractions x. In (2), $d\Delta\sigma$ denotes the spin-dependent cross section, which can be obtained by taking the difference of measurements with the (anti-)proton spins aligned and anti-aligned. The unpolarized cross section $d\sigma$ is determined by the sum of both measurements. We will explore the sensitivity of A_{LL} to different assumptions about polarized parton densities, in particular, the elusive gluon polarization. As for the unpolarized cross sections, we discuss theoretical uncertainties related to variations of the charm quark mass and the renormalization and factorization scales.

The paper is organized as follows: in Sec. 2 we briefly review the technical framework for hadroproduction of heavy flavors, set our notation, and introduce in some detail the charge asymmetry. Section 3 is devoted to numerical studies. First we define the phenomenological inputs and experimental cuts we assume for GSI-FAIR and J-PARC. Next, we give results for total and differential unpolarized charm cross sections and discuss their theoretical uncertainties. These results serve as a future benchmark to study the applicability of pQCD for charm production at $\sqrt{S} \simeq 10\,\mathrm{GeV}$. Then we present expectations for the polarized cross sections and charge and double spin asymmetries. We briefly summarize the main results in Sec. 4.

2 Technical Framework

The pQCD framework for single-inclusive heavy flavor production at NLO accuracy in both unpolarized and longitudinally polarized hadron-hadron collisions has been discussed in detail in Refs. [6] and [9], respectively. We can restrict ourselves to a brief summary of the aspects with particular relevance to our analysis.

2.1 The single-inclusive cross section

We are interested in the hadroproduction of a heavy quark Q [anti-quark $\bar{Q}$] with mass m_Q and four-momentum P_Q

$[P_{\bar{Q}}]$:

$$H_1(P_1)H_2(P_2) \to Q(P_Q)[\bar{Q}(P_{\bar{Q}})] + X. \quad (3)$$

X includes all other final-state particles such that (3) is inclusive with respect to the detected heavy quark. $P_{1,2}$ denote the momenta of the colliding hadrons $H_{1,2}$ and $S = (P_1 + P_2)^2$ the c.m.s. energy squared.

More specifically, P_Q can be parameterized in terms of the transverse momentum p_T, the rapidity y, and the azimuthal angle ϕ of the observed heavy quark Q,

$$P_Q = (m_T \cosh y, p_T \sin\phi, p_T \cos\phi, m_T \sinh y), \quad (4)$$

where the transverse mass is defined as $m_T = \sqrt{p_T^2 + m_Q^2}$ and $y = \frac{1}{2}\ln[(E + P_z)/(E - P_z)]$. Applying the factorization theorem, the unpolarized differential cross section for (3) can be written schematically as

$$\frac{d^2\sigma^Q}{dm_T^2 dy} = \sum_{ab} f_a^{H_1}(x_1,\mu_f) \otimes f_b^{H_2}(x_2,\mu_f) \otimes \frac{d^2\hat{\sigma}_{ab\to QX}(x_1,x_2,P_1,P_2,P_Q,\mu_f,\mu_r)}{dm_T^2 dy} \quad (5)$$

with the symbol $\otimes$ indicating a convolution. x_1 and x_2 are the fractions of P_1 and P_2 taken by the partons $f_a^{H_1}$ and $f_b^{H_2}$ with flavor a and b, respectively. The sum in Eq. (5) is to be performed over all contributing partonic channels $ab \to QX$ with $d\hat{\sigma}_{ab\to QX}$ the associated partonic cross sections.

The factorization of the cross section (5) into non-perturbative parton densities $f_{a,b}$ and short-distance cross sections requires the introduction of factorization and renormalization scales μ_f and μ_r, respectively. These scales are essentially arbitrary and usually chosen to be of the order of a hard momentum transfer characterizing the process under consideration. Any residual dependence of the right-hand-side (r.h.s.) of Eq. (5) on the actual choice for $\mu_{f,r}$ represents an important part of the uncertainties in the theoretical description of (3).

The basic framework outlined above carries over to the case of polarized hadron-hadron collisions as well. To obtain the spin-dependent cross section $d^2\Delta\sigma/dm_T^2 dy$ entering the experimentally relevant spin asymmetry A_{LL} defined in Eq. (2), the parton densities and hard scattering cross sections on the r.h.s. of Eq. (5) have to be replaced by their polarized counterparts $\Delta f_{a,b}$ and $d\Delta\hat{\sigma}_{ab\to QX}$, respectively.

Knowledge of higher-order corrections in the perturbative expansion of the partonic cross sections $d\hat{\sigma}_{ab\to QX}$ and $d\Delta\hat{\sigma}_{ab\to QX}$ is generally indispensable. On the one hand, in hadronic scattering they are often sizable, and, on the other hand, they are expected to reduce the artificial dependence on the choice of $\mu_{f,r}$. Also, higher-order corrections affect unpolarized and polarized cross sections differently and hence do not cancel in the ratio A_{LL}.

At $\mathcal{O}(\alpha_s^2)$, the LO approximation, the hadroproduction of heavy quarks proceeds through only two partonic channels

$$gg \to QX \text{ and } q\bar{q} \to QX \quad (6)$$

where $X = \bar{Q}$. The $\mathcal{O}(\alpha_s)$ radiative corrections to (6) comprise additional real gluon emission, $X = \bar{Q}g$, as well as one-loop (virtual) contributions. In addition, a new type of subprocess, gluon-[anti]quark-scattering, $gq[\bar{q}] \to QX$ has to be considered at NLO. A detailed account of the calculation of the relevant matrix elements, the required loop and phase-space integrations, and the cancellation of singularities is given in Refs. [6] and [9].

Since m_Q acts as an effective cut-off for collinear singularities, also total heavy quark yields are amenable to pQCD. They are obtained by integrating (5) over the entire phase-space using

$$\int_{m_Q^2}^{S/4} dm_T^2 \int_{-\cosh^{-1}\sqrt{S}/(2m_T)}^{\cosh^{-1}\sqrt{S}/(2m_T)} dy = \int_{-\frac{1}{2}\ln\frac{1+\beta}{1-\beta}}^{\frac{1}{2}\ln\frac{1+\beta}{1-\beta}} dy \int_{m_Q^2}^{S/(4\cosh^2 y)} dm_T^2, \quad (7)$$

where $\beta \equiv \sqrt{1 - 4m_Q^2/S}$. Alternatively, one can first derive the so-called "scaling functions", $[\Delta]\hat{\sigma}_{ab}(s, m_Q^2)$, as a function of the partonic c.m.s. energy s by integrating the partonic cross sections $d[\Delta]\hat{\sigma}_{ab\to QX}$ [6,9], which then in turn have to be combined with the appropriate combination of parton densities. We note that the experimental determination of the total cross section always involves some extrapolation beyond the accessible ranges in p_T and y and is therefore less reliable and useful than differential rates in testing pQCD predictions. In our numerical studies for J-PARC and GSI-FAIR we will therefore mainly focus on differential cross sections, which are also relevant for the charge asymmetry.

2.2 The charge asymmetry

At the LO approximation the processes (6) relevant for heavy flavor production do not discriminate between a produced heavy quark Q and a heavy anti-quark $\bar{Q}$. Hence, at any given point (p_T, y) in phase-space the yields (5) for Q and $\bar{Q}$ are identical.

Radiative corrections change this picture and give rise to the charge asymmetry A_C, defined in Eq. (1). Any measurement of A_C will directly probe and perhaps improve our understanding of QCD dynamics beyond the LO. So far this higher-order effect has received relatively little attention [17,18,19] but was recently measured for the first time in case of top production at CDF [20], the asymmetry exceeding the few percent predicted in [18] with large experimental uncertainties though. We will explore the prospects of accessing A_C in pp and $\bar{p}p$ collisions at J-PARC and GSI-FAIR, respectively. Due to the relatively low c.m.s. energies available, we have to limit ourselves to charm quark production. Given that longitudinally polarized beams and targets are a viable option, we also explore the polarized charge asymmetry, which we define as in Eq. (1) with the cross sections $d\sigma^{Q[\bar{Q}]}$ replaced by their polarized counterparts $d\Delta\sigma^{Q[\bar{Q}]}$.

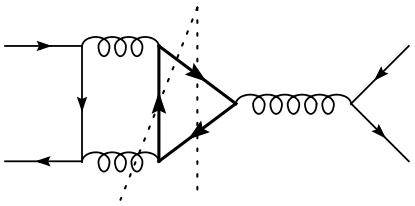

Fig. 1. Sample $q\bar{q}$ cut diagram contributing to A_C.

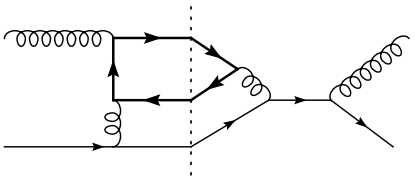

Fig. 2. Sample gq cut diagram contributing to A_C.

At NLO the charge asymmetry receives only a very limited number of contributions. Instead of making use of the results available in the literature [6,9], we chose to recalculate the numerator of A_C from scratch in both the unpolarized and polarized case[1]. The origin of A_C resides in the Abelian (QED) part of the higher order processes and relates to the interference between amplitudes which are relatively odd under the exchange of Q and $\bar{Q}$. The gluon-gluon fusion process in (6) is evidently charge symmetric also beyond the LO and does not contribute to A_C. Also non-Abelian amplitudes involving the triple-gluon vertex depend only on $Q+\bar{Q}$ and lead to contributions which are symmetric under exchanging Q and $\bar{Q}$. Upon close examination of the remaining amplitudes for the $q\bar{q}$ and gq $[g\bar{q}]$ initiated subprocesses at NLO, one finds that only such "cut diagrams" contribute which have three vertices on both the heavy and light quark line. In case of the virtual loop corrections to the LO $q\bar{q}$ process, only the interference of the box diagrams with the Born amplitude contributes. Examples of cut diagrams relevant for the computation of A_C and ΔA_C are depicted in Figs. 1 and 2.

This observation can be readily understood. To this end, let us write the partonic subprocess cross section $d\hat{\sigma}_{ab\to QX}$ as the sum of the interference contributions of all contributing amplitudes labeled by the indices i,j

$$d\hat{\sigma}_{ab\to QX} = K_{ab}\sum_{ij}\mathcal{M}_i\mathcal{M}_j^*\Big|_{ab\to QX}. \tag{8}$$

For simplicity, pre-factors such as the spin and color averages are mapped into K_{ab}. Phase-space integration for all unobserved partons is implicitly understood in (8). Expressions similar to (8) hold for polarized partonic cross sections $d\Delta\hat{\sigma}_{ab\to QX}$ as well as for $ab\to\bar{Q}X$. For the numerator of A_C we have to examine the difference

$$\Delta_{ij} = \mathcal{M}_i\mathcal{M}_j^*\Big|_{ab\to QX} - \mathcal{M}_i\mathcal{M}_j^*\Big|_{ab\to\bar{Q}X} \tag{9}$$

for all i,j. By interchanging Q and $\bar{Q}$, the Dirac structure relevant for $\mathcal{M}_i\mathcal{M}_j^*$ changes sign for an odd number of propagators in the heavy quark trace and otherwise remains the same. The color structure is invariant, except for $\mathrm{Tr}[T_kT_lT_m] = (d_{klm}+if_{klm})/4$ which contains a symmetric and an anti-symmetric piece, $d_{klm}=d_{mlk}$ and $f_{klm}=-f_{mlk}$, respectively.

Combining everything, only those cut diagrams with three vertices on both the heavy and the light quark line, cf. Figs. 1 and 2, contribute to A_C, and one finds [18]

$$\Delta_{ij} = \frac{1}{8}(d_{klm})^2\widetilde{\mathcal{M}_i\mathcal{M}_j^*}\Big|_{ab\to QX}, \tag{10}$$

with $(d_{klm})^2 = 40/3$. $\widetilde{\mathcal{M}_i\mathcal{M}_j^*}$ denotes the interference of the two amplitudes with the QCD color structure taken aside, and is the same (up to pre-factors) as for corresponding QED processes [16], e.g, $e^+e^-\to\mu^+\mu^-\gamma$. Let us mention that there is a similar effect in the QCD scale evolution of parton densities at next-to-next-to-leading order (NNLO) also proportional to $(d_{klm})^2$ and leading to a strange quark asymmetry $s(x)\neq\bar{s}(x)$ [21].

All contributions to the numerator of A_C at $\mathcal{O}(\alpha_s^3)$ are free of ultraviolet as well as collinear singularities as a consequence of the symmetry of the LO processes (6) under exchanging Q and $\bar{Q}$. Infrared (IR) singularities appear in both real gluon emission and virtual loop corrections to the LO $q\bar{q}$ process and cancel in the sum. Effectively this implies that the NLO matrix elements only contain the charge asymmetry at LO approximation. As in [6,9] we use dimensional regularization to deal with IR poles in intermediate steps of the calculation. In [18] a small gluon energy E^g_{cut} was used to cut off IR singularities. While the charge asymmetry also appears in the limit $m_Q\to 0$, it vanishes for the total heavy quark cross section as a consequence of charge conjugation invariance.

In Sec. 3.3 we give some quantitative predictions for A_C and ΔA_C at J-PARC and GSI-FAIR. Due to the low c.m.s. energies, gluons are much less abundant than at high-energy colliders. Since gluon-gluon fusion only contributes to the denominator of A_C, the prospects for studying A_C can be in fact more favorable at GSI-FAIR or J-PARC than at colliders like the TeVatron or the LHC. Here, gluon-gluon fusion is by far the dominant mechanism for heavy quark production, and one has to find suitable corners of phase-space to make A_C experimentally accessible. One important possibility is top quark production [18,19,20], which receives important contributions from $q\bar{q}$ annihilation also at large S thanks to the sizable m_Q.

3 Phenomenological Applications

Before turning to the prospects of heavy flavor physics at GSI-FAIR and J-PARC, we quickly review the information on charm production in pp collisions at c.m.s. energies below $\sqrt{S}=50\,\mathrm{GeV}$ gathered so far. Figure 3 shows the available data [22] compared to our calculations at NLO accuracy using different values of the charm quark

[1] The lengthy expressions are available upon request from the authors.

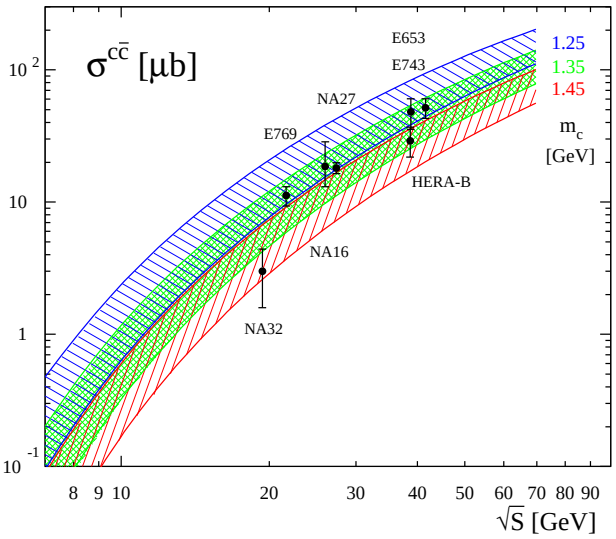

Fig. 3. Experimental results [22] for the total charm production cross section at fixed-target energies compared to NLO pQCD calculations for three different values of the charm quark mass m_c. In each case, the shaded band indicates the theoretical uncertainties from varying $\mu = \mu_r = \mu_f$ in the range $m_c \leq \mu \leq 2m_c$.

mass and scales $\mu = \mu_f = \mu_r$ in Eq. (5). As can be seen, uncertainties from small variations of m_c are as important as scale ambiguities, and both combined can lead to almost an order of magnitude change in the total charm yield at $\sqrt{S} \simeq 10 \div 20\,\text{GeV}$. From Fig. 3 one can also infer that the theoretical uncertainties become somewhat less pronounced with increasing c.m.s. energy.

Although most experimental results can be described with the same choice of m_c and scale μ, there is a clear need for further precise measurements, in particular closer to threshold, below the result of NA32, which does not line up so well with other experiments. GSI-FAIR and J-PARC, to which we shall turn now, can explore this energy range in the future.

3.1 Phenomenological inputs and experimental cuts

The part of the future GSI-FAIR accelerator complex amenable to pQCD studies is an asymmetric proton-antiproton collider option proposed by the PAX collaboration [14] with maximum beam energies for protons and antiprotons of 3.5 GeV and 15 GeV, respectively, resulting in a c.m.s. energy of about $\sqrt{S} = 14.5\,\text{GeV}$. Studies of methods to polarize both beams either longitudinally or transversely are currently pursued [14]. The PAX detector will have nearly full azimuthal acceptance and a polar angle coverage from 5 to 130 degrees is envisioned [14,23].

The proton accelerator at J-PARC, which will reach up to 50 GeV beam energy, is currently under construction, and the hadron physics programme will commence in the near future at a c.m.s. energy of about $\sqrt{S} = 10\,\text{GeV}$ with both beam and target being unpolarized. We also consider longitudinally polarized collisions, which are a conceivable upgrade of the J-PARC facility in the future [13]. Since not very much is known about the experimental set-up at this stage, we assume a forward spectrometer geometry with a 200 mrad acceptance, similar to the one used by the COMPASS experiment at CERN.

Since the details of charm detection in experiment are not yet available, we will perform all our calculations on the charm quark level, i.e., we do not attempt to model the hadronization of charm quarks into charmed mesons and their subsequent decays. For the PAX experiment, however, identification of open charm events most likely proceeds through the detection of decay muons for which a lower limit on their momentum of $p_\mu = 1\,\text{GeV}$ is required [14,23]. Therefore we impose a similar cut on the laboratory momentum of the primary charm quark in all our calculations for GSI-FAIR.

In all unpolarized calculations at LO and NLO accuracy we use the CTEQ6L1 and CTEQ6M parton distribution functions [24] and the corresponding LO and NLO values for the strong coupling, respectively. Unless stated otherwise, the GRSV "standard" set of helicity-dependent parton densities [25] is used in the computation of polarized cross sections and the charge and spin asymmetries. Since $m_c = 1.35\,\text{GeV}$ provides a good description of most of the data shown in Fig. 3, we make this our default choice for the charm quark mass.

3.2 Expectations for charm production cross sections

Figure 4 shows our expectations for the unpolarized charm production cross section (5) at GSI-FAIR at LO and NLO accuracy, integrated over transverse momentum $p_T > p_T^{\min}$ and the angular acceptance of $5^\circ \leq \theta_c \leq 130^\circ$ for PAX. The shaded bands indicate the theoretical uncertainties when the factorization and renormalization scales are varied simultaneously in the range $m_T^{\min} \leq \mu_f = \mu_r \leq 2m_T^{\min}$. Also shown in Fig. 4 are the "K-factors", the ratio of the NLO and LO cross sections, for two choices of scales $\mu_f = \mu_r$ and the fractional contributions of the different partonic channels σ_{ij}^c to the NLO cross section.

Besides the sizable dependence on the scales $\mu_{f,r}$, there is also a similar uncertainty due to the choice of m_c in the region $p_T^{\min} \lesssim 1\,\text{GeV}$, in line with the observations for the total charm yields in Fig. 3. For $p_T^{\min} \gtrsim 2\,\text{GeV}$, however, varying m_c in the range $1.25\,\text{GeV} \leq m_c \leq 1.45\,\text{GeV}$ has a negligible impact on the cross section shown in the upper panel of Fig. 4. It is worth to notice that there is only a rather marginal reduction in the scale ambiguity when going from the LO to the NLO approximation. This is not unexpected for experiments with limited c.m.s. energies, and similar observations have been made for single-inclusive hadron production [26]. From the lower panel of Fig. 4 one can infer that the quark-antiquark annihilation subprocess is the most important contribution to the cross section. This can be readily understood since quarks and antiquarks are both "valence" partons in the proton and antiproton, respectively, and from the fact that one probes

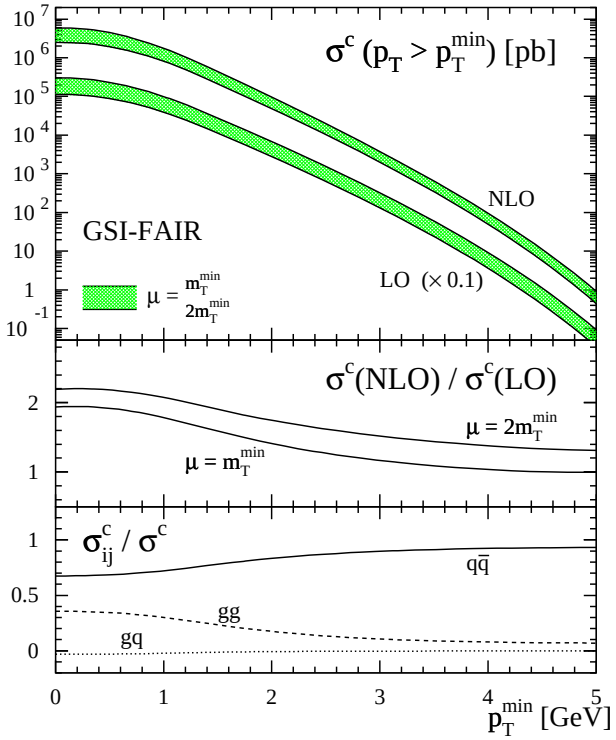

Fig. 4. upper panel: LO and NLO unpolarized charm cross section at GSI-FAIR, integrated over $p_T > p_T^{\min}$ and the angular acceptance $5^\circ \leq \theta_c \leq 130^\circ$, using $m_c = 1.35\,\text{GeV}$. The shaded bands indicate the uncertainties from varying $\mu = \mu_r = \mu_f$ in the range $m_T^{\min} \leq \mu \leq 2m_T^{\min}$; middle panel: ratio of the NLO and LO cross sections ("K-factor"); lower panel: fractional contribution of the different partonic channels σ_{ij}^c to the NLO cross section σ^c for $\mu = \sqrt{2}m_T^{min}$.

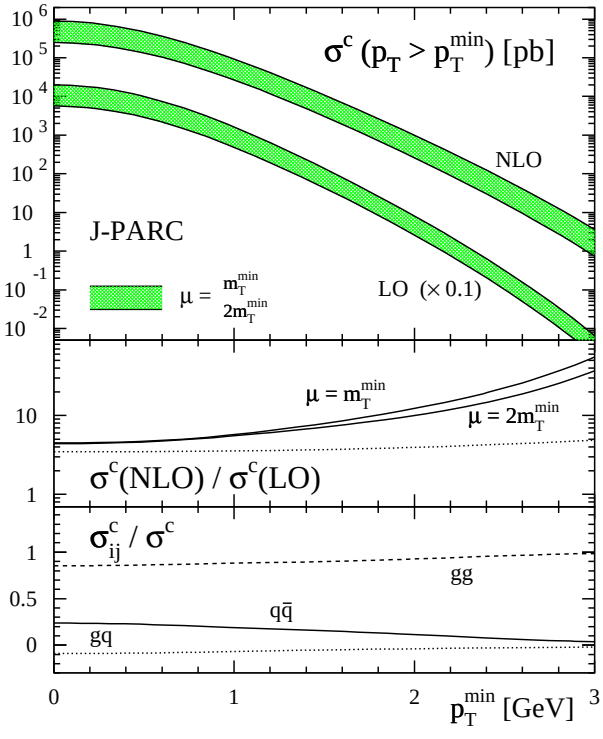

Fig. 5. Same as in Figure 4, but now for J-PARC kinematics.

fairly large momentum fractions $x_{1,2} \gtrsim 0.1$. The genuine NLO quark-gluon subprocess is negligible in the entire p_T range shown.

The corresponding results for J-PARC are summarized in Fig. 5. There are striking differences compared to the result for GSI-FAIR shown in the previous figure. The dependence of the charm cross section on unphysical scales $\mu_{f,r}$ is even larger here and does not improve when NLO corrections are included. This can be taken as a strong indication that higher order terms in the perturbative series are very important. Hopefully, a resummation of the leading terms to all orders in α_s will tame the scale ambiguities. Secondly, the size of the NLO corrections compared to the LO term, displayed in the middle panel of Fig. 5, seems to be beyond control. Most of the pathological behavior of the K-factor at large $p_T^{\min}$ can be attributed to the differences in the LO and NLO gluon distributions at large $x_{1,2}$, where they are basically unconstrained by data [24]. If one uses NLO parton densities in the calculation of the LO cross section, the K-factor does not show such a sharp rise, though it remains large (dotted curve in Fig. 5). Despite the rather large $x_{1,2}$ values probed at J-PARC, and contrary to what happens in $\bar{p}p$ collisions at GSI-FAIR, the gluon-gluon fusion subprocess is by far the dominant mechanism to produce the charm quark. We also note that varying m_c in the range $1.25\,\text{GeV} \leq m_c \leq 1.45\,\text{GeV}$ has a somewhat bigger impact on the cross sections displayed in the upper panel of Fig. 5 than in case of GSI-FAIR due to the smaller c.m.s. energy.

Figures 4 and 5 already demonstrate the potential of future low energy $\bar{p}p$ and pp experiments in further constraining quark and gluon distributions, respectively, in the medium-to-large x region, difficult to access at high energy colliders. They also show, however, that the pQCD framework can not be taken for granted in this energy regime, and its applicability has to be carefully scrutinized first by comparing the theoretical expectations with data.

Figure 6 shows the corresponding longitudinally polarized cross sections at NLO accuracy for GSI-FAIR and J-PARC, respectively. Instead of giving also the LO results [the K-factors are smaller than in the unpolarized case, between 1.5 and 2 (2 and 4) for GSI-FAIR (J-PARC)], we chose to display the dependence of the polarized cross sections on m_c. Since J-PARC can cover only a smaller range in p_T than GSI-FAIR due to the smaller $\sqrt{S}$, the mass effects are more important here. The fractional contributions of the different subprocesses are very similar to those shown in Fig. 4 for GSI-FAIR and strongly dependent on the size of the polarized gluon distribution in case of J-PARC, as can be expected already from the lower panel of Fig. 5. We note that at J-PARC kinematics, the

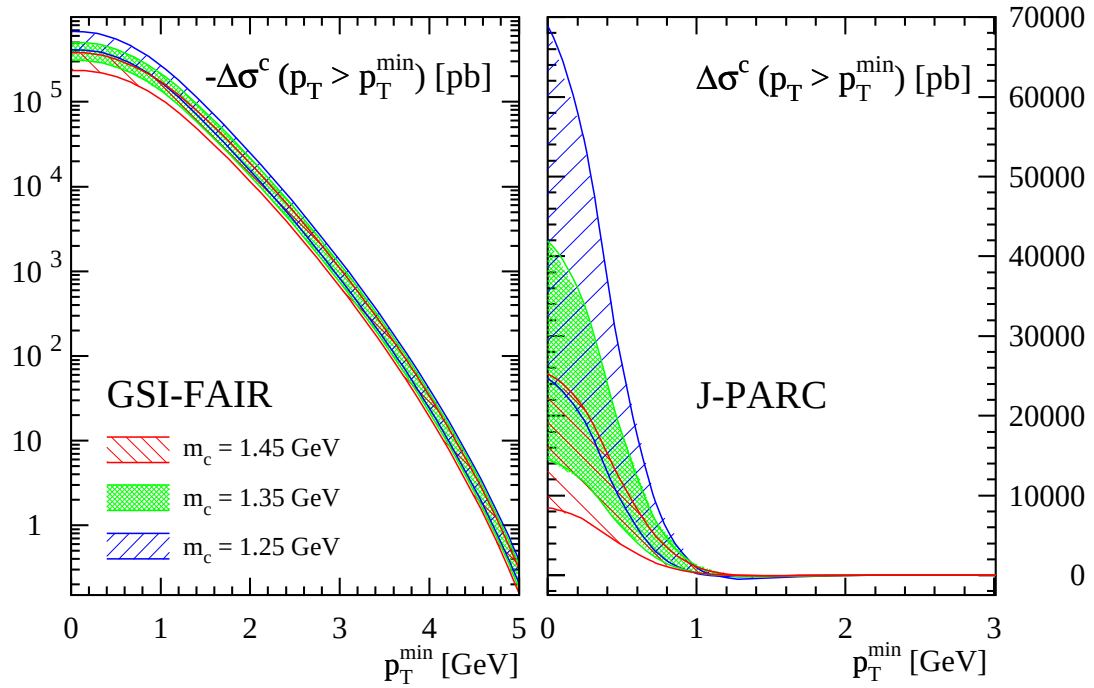

Fig. 6. Expectations for the longitudinally polarized cross section for charm production at GSI-FAIR (left panel) and J-PARC (right panel), using the GRSV "standard" set [25]. Note that the results on the left hand side are for $-\Delta\sigma$. The scale uncertainty is shown for three different choices of m_c, varying $\mu = \mu_r = \mu_f$ in the range $m_T^{\min} \leq \mu \leq 2m_T^{\min}$.

polarized cross section exhibits a node at $p_T^{\min} \simeq 1\,\text{GeV}$ if the GRSV "standard" parton densities are used in the calculation.

3.3 The unpolarized and polarized charge asymmetry

We now turn to a detailed discussion of the charge asymmetry A_C defined in Eq. (1) and Sec. 2.2. We show expectations for the size of the effect and discuss the theoretical uncertainties due to variations of $\mu_{f,r}$ and m_c. All results are presented as a function of the c.m.s. rapidity y of the heavy (anti-)quark, which is related to the rapidity in the laboratory frame y_{lab} by a simple additive boost. Positive rapidities refer to the direction of the anti-proton and proton beam at GSI-FAIR and J-PARC, respectively. Recall that rapidity y and pseudo-rapidity η are not the same for massive particles. The relation between y and the scattering angle θ_c of the heavy quark depends both on p_T and m_c

$$\cos\theta_c = \left(\sqrt{\frac{m_T^2}{1-\tanh^2 y}}\tanh y\right) \Big/ \sqrt{\frac{m_T^2}{1-\tanh^2 y} - m_c^2} \tag{11}$$

while $\cos\theta_c = \tanh\eta$. Therefore, angular cuts imposed upon the heavy quarks by the experiments do not translate in simple, p_T independent cuts for rapidity-dependent differential cross sections.

The upper panels of Figs. 7 and 8 show our expectations for the unpolarized charge asymmetry A_C at $\mathcal{O}(\alpha_s^3)$

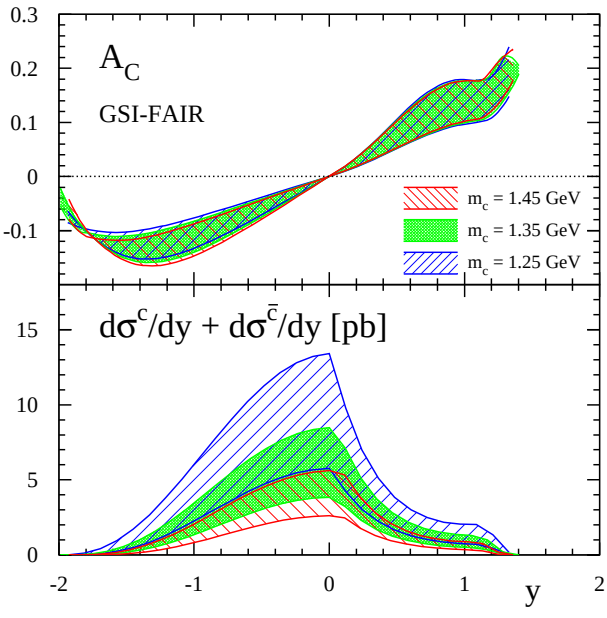

Fig. 7. The unpolarized charge asymmetry A_C (upper panel) and the NLO c.m.s. rapidity-dependent differential charm plus anti-charm cross section $d\sigma^c/dy + d\sigma^{\bar{c}}/dy$ (lower panel) for GSI-FAIR. The scale uncertainty is shown for three different choices of m_c, varying $\mu = \mu_r = \mu_f$ in the range $m_c \leq \mu \leq 2m_c$.

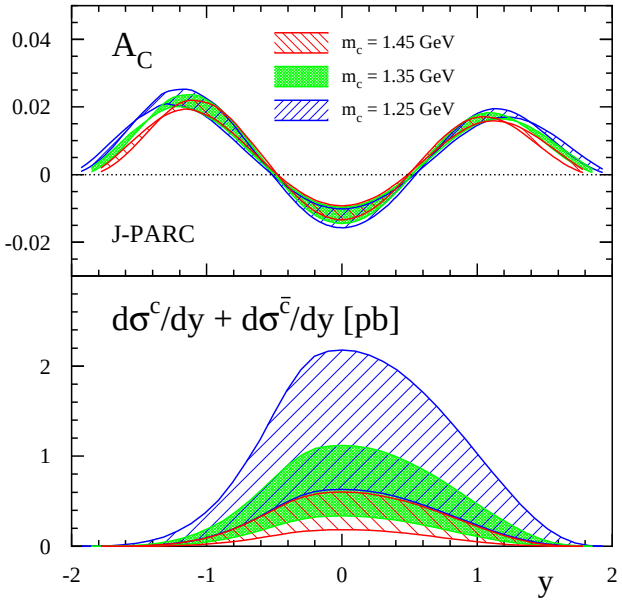

Fig. 8. Same as in Fig. 7 but for J-PARC kinematics.

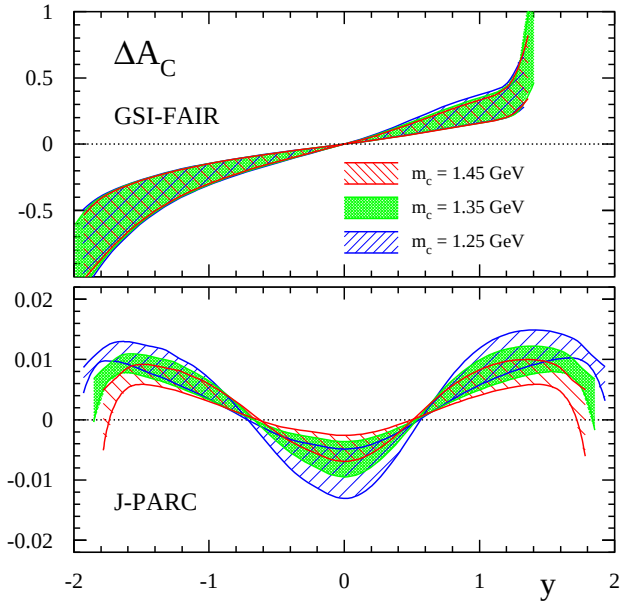

Fig. 9. Same as in the upper panels of Figs. 7 and 8 but now for the polarized charge asymmetry ΔA_C.

for charm quarks at GSI-FAIR and J-PARC, respectively, using the phenomenological inputs and experimental acceptance cuts specified in Sec. 3.1. The results for A_C are largely independent of the choice for the charm quark mass m_c, in contrast to the sizable mass dependence observed for the NLO c.m.s. rapidity-dependent differential cross sections for the sum of charm and anti-charm production (lower panels), which enters in the denominator of A_C in Eq. (1).

Note that the c.m.s. rapidity y and the experimentally relevant rapidity y_{lab} in the laboratory frame are simply related by $y_{lab} = y - 0.737$ and $y_{lab} = y + 2.334$ for GSI-FAIR and J-PARC, respectively. The scale $\mu_{f,r}$ dependence partially cancels out in A_C, as can be seen by comparing the upper and lower panels of Figs. 7 and 8. A residual dependence on $\mu_{f,r}$ is not surprising since the numerator of A_C at $\mathcal{O}(\alpha_s^3)$ is effectively a LO approximation. It vanishes at $\mathcal{O}(\alpha_s^2)$ and is free of collinear singularities. Also note that the sharp drop of $d\sigma^c/dy + d\sigma^{\bar{c}}/dy$ in the lower panel of Fig. 7 is due to the cut imposed on the momentum of the heavy (anti-)quark, $p_{lab} > 1\,\mathrm{GeV}$.

Figure 9 shows our results for the longitudinally polarized charge asymmetry ΔA_C defined as in Eq. (1), but with all cross sections $d\sigma$ replaced by their helicity dependent counterparts $d\Delta\sigma$. Again, the scale uncertainty is shown for three different choices of m_c, varying $\mu = \mu_r = \mu_f$ in the range $m_c \leq \mu \leq 2m_c$. All results are obtained with the GRSV "standard" set [25] of spin-dependent parton densities. As in the unpolarized case, the mass dependence largely drops out in ΔA_C, in particular for GSI-FAIR, but a residual scale $\mu_{f,r}$ ambiguity remains.

Since the mass and scale dependence of $d\Delta\sigma^c/dy + d\Delta\sigma^{\bar{c}}/dy$ is qualitatively very similar to the corresponding unpolarized cases shown in the lower panels of Figs. 7 and 8, we refrain from giving these results here. Instead, we shall discuss the significant dependence of both numerator and denominator of ΔA_c on the choice of a particular set of polarized parton densities.

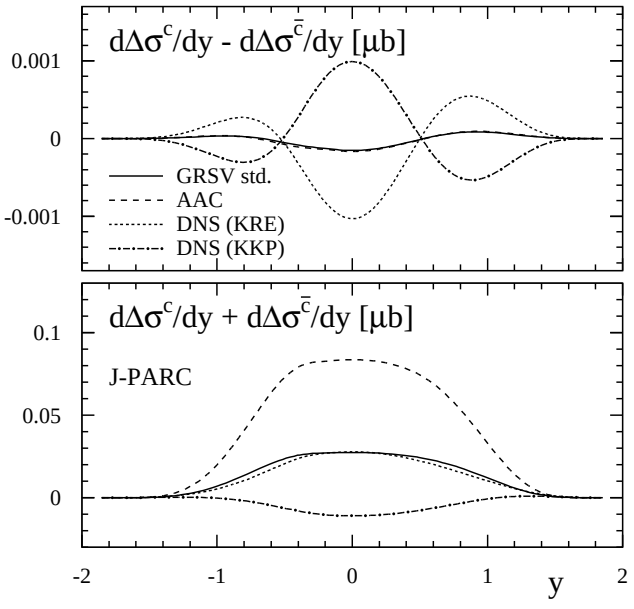

Fig. 10. Numerator (upper panel) and denominator (lower panel) of the polarized charge asymmetry ΔA_C at J-PARC, calculated with different sets of polarized parton densities.

Figure 10 shows the numerator and the denominator of the polarized charge asymmetry ΔA_C at J-PARC, ob-

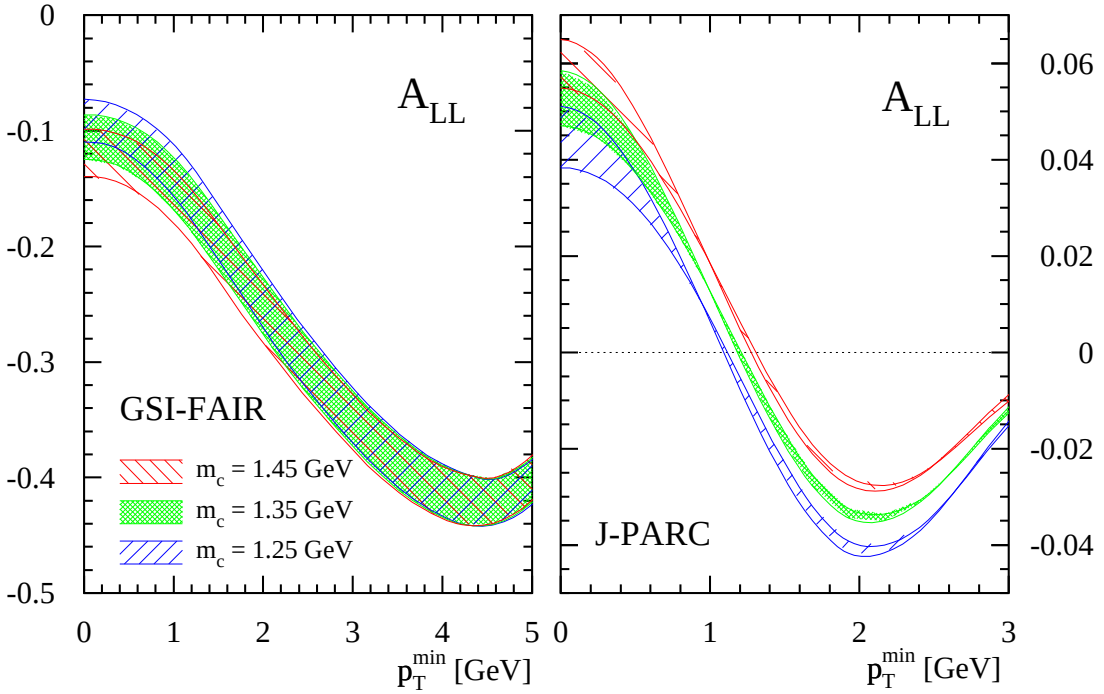

Fig. 11. The integrated double-spin asymmetry A_{LL} as function of $p_T^{\min}$ at NLO accuracy for GSI-FAIR (left panel) and J-PARC (right panel) using the GRSV "standard" distributions and the same experimental cuts as before. The scale uncertainty is shown for three different choices of m_c, varying $\mu = \mu_r = \mu_f$ in the range $m_T^{\min} \leq \mu \leq 2m_T^{\min}$.

tained with different sets of polarized parton densities. Apart from our default set, GRSV "standard", we also use the sets of AAC [27] and DNS [28]. The latter is based on an analysis using also data from polarized semi-inclusive deep-inelastic scattering. Two different choices of parton-to-hadron fragmentation functions have been made in the DNS analysis, and the two resulting sets, labeled as DNS (KRE) and DNS (KKP) in Fig. 10, differ mainly in the sea quark content, in particular, $\Delta\bar{u}$, which has opposite sign in both sets. The positive polarization of $\Delta\bar{u}$ in DNS (KKP), unlike in all others sets of spin-dependent parton densities, is responsible for the opposite sign of $d\Delta\sigma^c/dy \pm d\Delta\sigma^{\bar{c}}/dy$ obtained with DNS (KKP). In the denominator of ΔA_C, gluon-gluon fusion does not drop out and can make a significant contribution depending on the amount of gluon polarization Δg. The set with the largest Δg, AAC, gives the largest cross section. The other three sets have relatively small gluon distributions and quark-antiquark annihilation is equally important. On the other hand, different sets of polarized parton densities have only very limited impact on the results for $d\Delta\sigma^c/dy \pm d\Delta\sigma^{\bar{c}}/dy$ and ΔA_C for GSI-FAIR. This can be expected, since in $\bar{p}p$ collisions at small $\sqrt{S}$ one predominantly probes the fairly well constrained valence quark distributions, and uncertainties in the polarized sea-quark and gluon densities do not matter much.

Finally, we note that *without* taking into account any experimental cuts, A_C and ΔA_C are anti-symmetric functions in the c.m.s. rapidity for $\bar{p}p$ collisions, as can be anticipated from Figs. 7 - 9 (which, however, do include certain acceptance cuts). Similarly, A_C and ΔA_C are symmetric in c.m.s. rapidity for pp experiments. This is a consequence of the anti-symmetric and symmetric initial states $\bar{p}p$ and pp, respectively. The charge asymmetry on the partonic level for the dominant $q\bar{q}$ subprocess implies that Q is preferentially emitted into the direction of q and $\bar{Q}$ into the direction of $\bar{q}$. As was explained in [18], in pp collisions one then finds an excess of centrally produced $\bar{Q}$, while Q dominates at large absolute rapidities. This is also what we observe for J-PARC in Figs. 8 and 9. The size of A_C and ΔA_C for pp collisions at J-PARC is significantly smaller than for $\bar{p}p$ collisions at GSI-FAIR, simply because of the fact that for the relevant $q\bar{q}$ subprocess both partons are valence quarks in $\bar{p}p$, greatly enhancing its relative contribution. When integrated over rapidity and without any kinematical restrictions, A_C and ΔA_C vanish, and the total yields of charm and anti-charm quarks are the same.

3.4 Expectation for longitudinal spin asymmetries

Experiments usually present their spin-dependent measurements in terms of spin-asymmetries rather than polarized cross sections. The double-spin asymmetry A_{LL}, defined in Eq. (2), has the advantage that many experimental uncertainties cancel in the ratio, in particular, it is not required to determine the absolute normalization of the helicity dependent cross sections. Also, theoretical uncertainties may cancel to some extent in A_{LL}. However, before exploiting this, one has to make sure that pQCD is

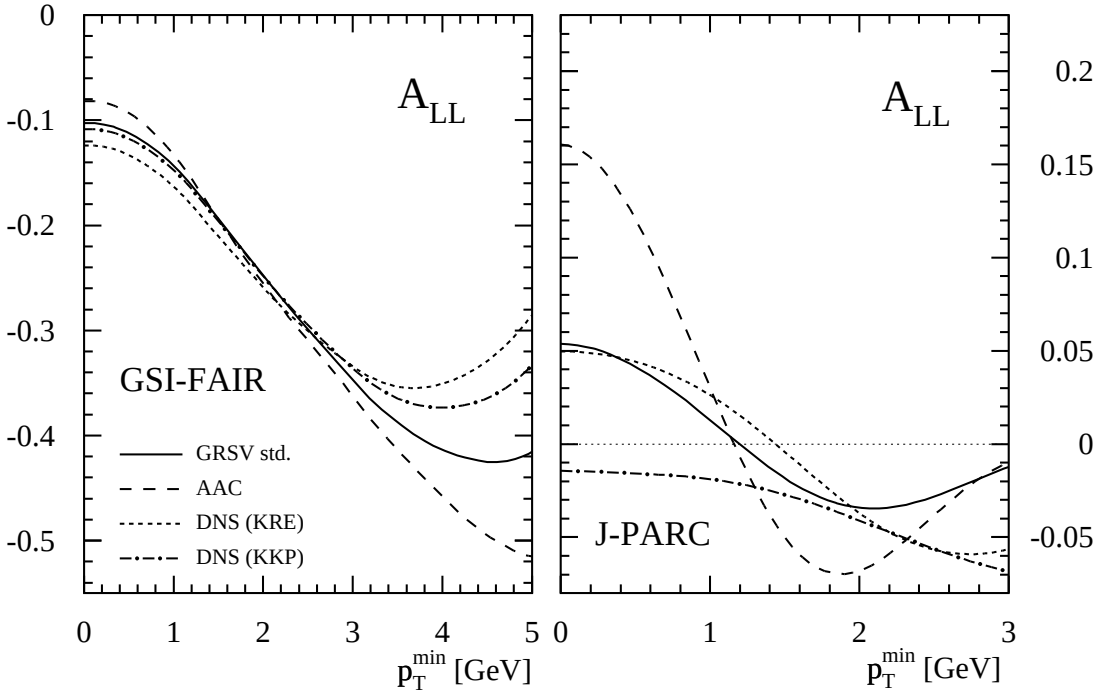

Fig. 12. As in Fig. 11 but now comparing the results obtained with different sets of polarized parton densities using $m_c = 1.35\,\mathrm{GeV}$ and $\mu_f = \mu_r = \sqrt{2}m_T^{\mathrm{min}}$.

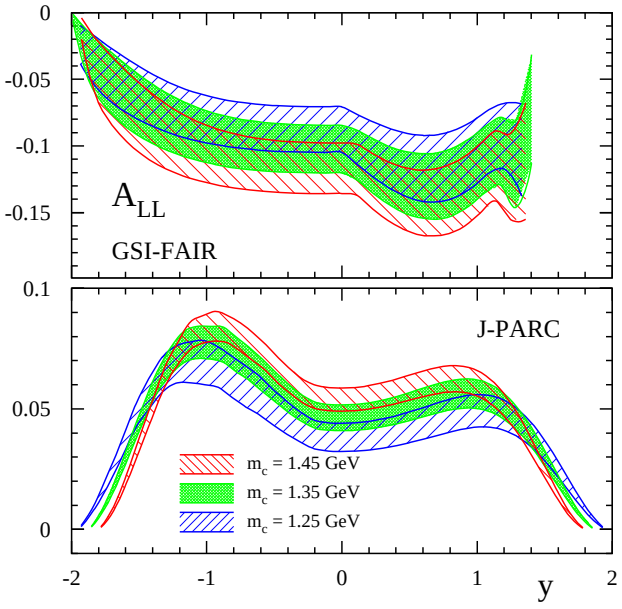

Fig. 13. As in Fig. 11 but now as function of the c.m.s. rapidity y. The scales $\mu_{f,r}$ are varied in the range $m_c \leq \mu_f = \mu_r \leq 2m_c$.

applicable in the relevant kinematical regime by comparing, for instance, the unpolarized cross section with data.

Figure 11 shows the integrated double-spin asymmetry A_{LL} as function of p_T^{min} at NLO accuracy for GSI-FAIR (left panel) and J-PARC (right panel), using the GRSV "standard" distributions and the same experimental cuts as for the underlying cross sections shown in Figs. 4 - 6. As usual, the scale uncertainty is shown for three different choices of m_c, varying $\mu = \mu_r = \mu_f$ in the range $m_T^{\mathrm{min}} \leq \mu \leq 2m_T^{\mathrm{min}}$. As can be seen, there is still a significant scale ambiguity and, in case of J-PARC, also a dependence on m_c. We refrain from showing LO results, but we note that because NLO corrections tend to be larger in the unpolarized case, as discussed above, A_{LL} is typically reduced by a factor of about two when NLO corrections are included.

The sensitivity of A_{LL} to different sets of polarized parton distributions is studied in Fig. 12. As expected, the differences are small for GSI-FAIR which mainly probes the fairly well known valence distributions. Only at large p_T^{min}, which corresponds to currently unexplored momentum fractions $x_{1,2} \to 1$, some differences are noticeable. At J-PARC, expectations for A_{LL} depend much more on the choice of spin-dependent parton densities, in line with the observations already made in the lower panel of Fig. 10.

Finally, in Fig. 13 we present the spin asymmetry as a function of the c.m.s. rapidity y and integrated over transverse momentum. The behavior of A_{LL} for GSI-FAIR in the upper panel for positive y is driven by the cut on the charm momentum $p_{lab} > 1\,\mathrm{GeV}$. Both mass and scale uncertainties do not cancel and remain significant.

4 Conclusions

We have performed a detailed study of the physics opportunities with open charm production at low c.m.s. energy $\bar{p}p$ and pp collisions at GSI-FAIR and J-PARC, respectively, including unpolarized and polarized cross sections and charge and spin asymmetries. All calculations are done at $\mathcal{O}(\alpha_s^3)$ accuracy, and theoretical uncertainties due to the choice of scales $\mu_{f,r}$ and the charm mass m_c are discussed in detail. In general, they turn out to be significant with the exception of the mass dependence of the charge asymmetries A_C and ΔA_C.

Measurements of all these quantities would further our understanding of the perturbative QCD framework and the nucleon structure expressed in terms of unpolarized and polarized parton densities. The latter are probed at large momentum fractions $x_{1,2}$, which are difficult to access at high-energy colliders. The charge asymmetry vanishes at $\mathcal{O}(\alpha_s^2)$ and hence is a clear probe of non-trivial QCD dynamics beyond the LO. Detailed comparisons between our theoretical expectations for unpolarized charm yields and future data will reveal to what extent perturbative methods are applicable in hadron-hadron collisions at $\sqrt{S} \approx 10 \div 15\,\mathrm{GeV}$ and will open up a window to perturbative resummations and/or the transition into the non-perturbative regime so far only little explored.

Acknowledgements

We are grateful to Marco Contalbrigo providing information about the GSI-FAIR PAX project. J.R. was supported by a grant of the "Cusanuswerk", Bonn, Germany. This work was supported in part by the BMBF, Germany.

References

1. For a recent review, see, e.g., J. Baines *et al.*, *Heavy Quark - Summary Report for the HERA-LHC Workshop Proceedings*, `hep-ph/0601164`, and references therein.
2. See, e.g., M. Cacciari, in proceedings of the *7th DESY Workshop on Elementary Particle Theory: Loops and Legs in Quantum Field Theory*, Zinnowitz, Germany, 2004, Nucl. Phys. B Proc. Suppl. **135** (2004) 61 and references therein.
3. See, e.g., A.D. Frawley *et al.*, *Heavy Flavor Working Group Report of RHIC II Science Workshop*, `http://www.bnl.gov/physics/rhicIIscience`, and references therein.
4. M. Cacciari, P. Nason, and R. Vogt, Phys. Rev. Lett. **95** (2005) 122001.
5. See, e.g., C. Aidala *et al.*, *Research Plan for Spin Physics at RHIC*, 2005, BNL report BNL-73798-2005.
6. W. Beenakker, H. Kuijf, W.L. van Neerven, and J. Smith, Phys. Rev. **D40** (1989) 54; P. Nason, S. Dawson, and R.K. Ellis, Nucl. Phys. **B303** (1988) 607; Nucl. Phys. **B327** (1989) 49; *ibid.* **B335** (1989) 260; W. Beenakker, W.L. van Neerven, R. Meng, G.A. Schuler, and J. Smith, Nucl. Phys. **B351** (1991) 507; M.L. Mangano, P. Nason, and G. Ridolfi, Nucl. Phys. **B373** (1992) 295.
7. R.K. Ellis and P. Nason, Nucl. Phys. **B312** (1989) 551; J. Smith and W.L. van Neerven, Nucl. Phys. **B374** (1992) 36; S. Frixione, M.L. Mangano, P. Nason, and G. Ridolfi, Nucl. Phys. **B412** (1994) 225.
8. E. Laenen, S. Riemersma, J. Smith, and W.L. van Neerven, Nucl. Phys. **B392** (1993) 162; *ibid.* **B392** (1993) 229; S. Riemersma, J. Smith, and W.L. van Neerven, Phys. Lett. **B347** (1995) 143; B.W. Harris and J. Smith, Nucl. Phys. **B452** (1995) 109.
9. I. Bojak and M. Stratmann, Phys. Rev. **D67**, 034010 (2003).
10. I. Bojak and M. Stratmann, Phys. Lett. **B433** (1998) 411; Nucl. Phys. **B540** (1999) 345; *ibid.* **B569** (2000) 694(E); A.P. Contogouris, G. Grispos, Z. Merebashvili, Phys. Rev. **D62** (2000) 114509; *ibid.* **D69** (2004) 019901(E).
11. M. Cacciari and M. Greco, Nucl. Phys. **B421** (1994) 530; M. Cacciari, M. Greco, and P. Nason, JHEP **9805** (1998) 007; M. Cacciari, S. Frixione, and P. Nason, JHEP **0103** (2001) 006.
12. For information on the planned GSI-FAIR facility, see: `http://www.gsi.de/fair`.
13. For information on the J-PARC facility, see: `http://j-parc.jp/index-e.html`.
14. GSI-PAX Collaboration, P. Lenisa and F. Rathmann (spokespersons), Technical Proposal, 2005, `hep-ex/0505054`; update of the Technical Proposal, 2006, `http://www.fz-juelich.de/ikp/pax`.
15. D. de Florian and W. Vogelsang, Phys. Rev. **D71** (2005) 114004; *ibid.* **D72** (2005) 014014.
16. F.A. Berends *et al.*, Nucl. Phys. **B63** (1973) 381; *ibid.* **B68** (1974) 541; Acta Phys. Polon. **B14** (1983) 413; R.W. Brown *et al.*, Phys. Lett. **B43** (1973) 403; S.J. Brodsky, C.E. Carlson, and R. Suaya, Phys. Rev. **D14** (1976) 2264.
17. R.W. Brown, D. Sahdev, and K.O. Mikaelian, Phys. Rev. Lett. **43** (1979) 1069; F. Halzen, P. Hoyer, and C.S. Kim, Phys. Lett. **B195** (1987) 74.
18. J.H. Kühn and G. Rodrigo, Phys. Rev. Lett. **81** (1998) 49; Phys. Rev. **D59** (1999) 054017.
19. M.T. Bowen, S.D. Ellis, and D. Rainwater, Phys. Rev. **D73** (2006) 014008; S. Dittmaier, P. Uwer, and S. Weinzierl, Phys. Rev. Lett. **98** (2007) 262002.
20. J. Weinelt, Masters Thesis, FERMILAB-MASTERS-2006-05, 2006.
21. S. Catani *et al.*, Phys. Rev. Lett. **93** (2004) 152003.
22. C. Lourenco and H.K. Wöhri, Phys. Rept. **433** (2006) 127.
23. Marco Contalbrigo, private communication.
24. J. Pumplin *et al.*, CTEQ Collaboration, JHEP **07** (2002) 012
25. M. Glück, E. Reya, M. Stratmann, and W. Vogelsang, Phys. Rev. **D63**, 094005 (2001).
26. B. Jäger, M. Stratmann, and W. Vogelsang, Eur. Phys. J. **C44** (2005) 533.
27. M. Hirai *et al.*, Asymmetry Analysis Collaboration, Phys. Rev. **D69** (2004) 054021.
28. D. de Florian, G.A. Navarro, and R. Sassot, Phys. Rev. **D71** (2005) 094018.